Multisine Excitation for ACPR Measurements*

Kate A. Remley

National Institute of Standards and Technology, RF Technology Division 813.01
325 Broadway; Boulder, CO 80305

Abstract — **We use a simulator to compare adjacent-channel power ratio (ACPR) measurements of a nonlinear device excited with various multisine signals to ACPR measurements of the same device excited with pseudorandom digital modulation. We examine four common types of multisine excitation, each with identical numbers of tones, tone-spacings, and nominal power levels, but with different magnitude and phase relationships between tones. We show that use of some common multisines may result in significant overestimation of the actual ACPR from the digitally modulated nonlinear device.**

I. Introduction

We investigate the use of some common multisine signals intended to approximate digitally modulated excitation in adjacent-channel power ratio (ACPR) measurements. We use time-domain simulations of representative RF signals to compare two modulation schemes: digital modulation employing quadrature-phase-shift keying (QPSK) and multisine signals. We subject a nonlinear device to both types of excitation and compare ACPR calculations to explore the validity of replacing a QPSK-modulated signal with multisine excitation. This direct and systematic comparison shows that multisines with a peak-to-average power ratio (PAPR) closer to that of the digital signal generally give better ACPR results. However, none of the multisines considered here reproduced ACPR with digital signal excitation in all cases.

Multisines consist of a collection of simultaneously generated sinewaves, typically with a constant frequency spacing Δf between sinewaves. They are often easier to generate than digital modulation, and characteristics such as peak-to-average power ratio are relatively easy to control. These qualities make them useful in applications such as system identification and model development [1-3], and for characterization of circuits or systems [4-6], among others. Additionally, nonlinear vector network analyzers (NVNAs) require the use of multisines for modulated signal measurements [2, 6]. For characterization of systems that incorporate nonlinear devices such as amplifiers, multisines represent an extension of the use of single- or two-tone signals for calculating distortion products [4]. Here, we assess various types of multisines in determinating one nonlinear system figure of merit, ACPR.

We use a bandpass multisine, a subset of the harmonically related multisines discussed in, for example, [1, 3]. Our bandpass multisine is given by

$$x(t) = \sum_{k=-(N-1)/2}^{(N-1)/2} A_k \cos\left(2\pi(f_c + k\Delta f)t + \phi_k\right), \qquad (1)$$

where we require the carrier frequency f_c to be an integer multiple of Δf, and N is the total number of sinewave components in the multisine.

The magnitude A_k and phase ϕ_k of each sinewave component of a multisine can be specified independently. The relationship between the phases of each sinewave component will have a particularly significant effect on the behavior of the multisine. We investigate multisines with four different magnitude/phase relationships between sinewave components: (1) constant phase and constant magnitude, (2) constant magnitude and random phase [2-4], (3) random magnitude and random phase [6], (4) constant magnitude and "Schroeder" phase [1]. The Schroeder multisine is one of a class of multisines in which the peak-to-average power ratio is minimized to better approximate realistic digitally modulated signals, as will be shown in the following sections. We analyze simulations with increasing numbers of sinewave components and with increasing average input power level.

II. Description

Our simulations were designed to approximate a digitally modulated signal with specifications similar to those in the IS-95 CDMA Cellular standard [7]. We chose a carrier frequency of 800 MHz (the CDMA forward link is 869-894 MHz and the reverse link is 824-849 MHz), a modulation bandwidth of 1.6 MHz and data rate of 25 ksymbols/s (the CDMA channel spacing is 1.2288 MHz with typical data rates of 19.2 or 28.8 ksymbols/s). We used QPSK modulation (currently used for the forward links of CDMA signals, while offset-QPSK (OQPSK) is used for the reverse links).

* Work of the National Institute of Standards and Technology, not subject to U.S. copyright.

US Government Work Not Protected by US Copyright.

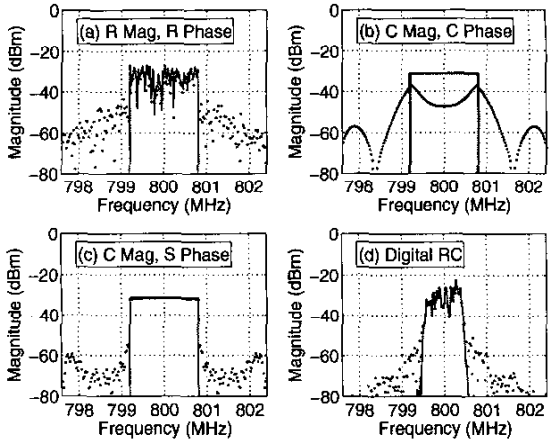

Figure 1: Spectrum before (lines) and after (dots) limiting of a 65-component multisine. (a) Random magnitude and phase. (b) Constant magnitude and phase. (c) Constant magnitude and Schroeder phase. (d) One pseudorandom QPSK-modulated 32-symbol digital signal using raised-cosine pulse shaping.

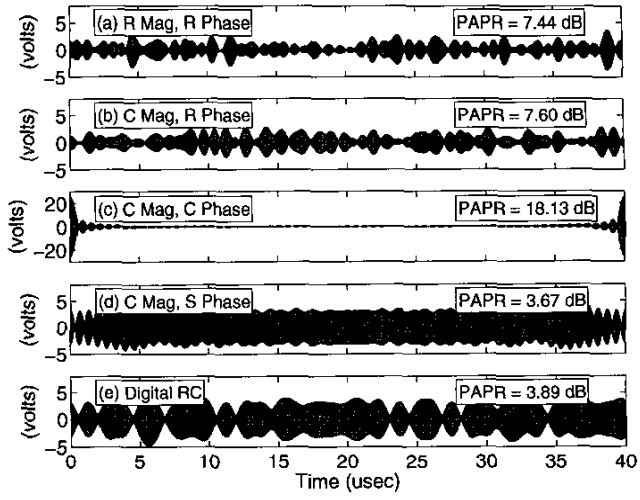

Figure 2: Time-domain representation of our four types of multisines. In this figure, each multisine has 65 sinewave components. (a) Random magnitude and phase; (b) Constant magnitude, random phase. (c) Constant magnitude, constant phase; (d) Constant magnitude, Schroeder phase; (e) The digital signal with raised-cosine filtering. Also shown are the values of peak-to-average power ratio (PAPR). Note the high PAPR [equal to 10log10(N)] in (c).

For our digital signal simulations, we used in-phase (I) and quadrature-phase (Q) non-return-to-zero (NRZ) pseudorandom bit streams. Each simulation consisted of 32 two-bit symbols. Due to the computational intensity, several simulations were carried out and averaged, as described in the following section. Noncausal raised-cosine pulse shaping (filtering) with $\alpha = 0.35$ was implemented over ±4 symbols (±7 symbols is often used in QPSK modulators [7]).

To approximate the digital signal with multisines, we restricted sinewave component placement to a 25 kHz grid in the 1.6 MHz modulation bandwidth. This limited the number of possible multisines to six: $N = 3, 5, 9, 17, 33,$ and 65.

To maximize computational accuracy (although not the efficiency), our simulations were performed at RF frequencies. Signals were generated in the time domain, where gain and limiting were applied, and then transformed to the frequency domain using the Fast-Fourier Transform (FFT). We avoided potential truncation or windowing effects [3] by simulating an entire period of the RF envelope: $1/\Delta f$ for the multisine case and an entire symbol pattern for the digital case.

For maximum efficiency in the FFT algorithm, we further required that the number of points n in the simulation be a power of two. We chose $n = 2^{19}$, corresponding to $f_{max} = n\Delta f/2 \approx 6.55$ GHz. This enabled us to characterize the output signal up to the fifth harmonic of the 800 MHz carrier. Identical simulation parameters were used for the digital case and all of the multisine cases, again for consistency, regardless of the number of sinewave components.

For the simulations corresponding to Figs. 1-5, we specified a total average input power of 0.2 W, applied a power gain of five, and hard-limited the signals to 3 V. We also carried out simulations using a soft limiter, whose transfer function is similar to that of many common memoryless amplifiers. The two limiter types are compared in Fig. 6.

Figure 1 shows typical spectral results for both multisine and digital excitation: (a) a multisine with 65 random magnitude and phase components, (b) a multisine with 65 constant magnitude and phase components, (c) a multisine with 65 constant magnitude and Schroeder phase components, and (d) a pseudorandom digital signal with raised-cosine pulse shaping. Figure 2 shows a time-domain representation of all four types of multisines and the digital signal with raised-cosine pulse shaping. The envelope of the QPSK signal before pulse shaping has constant amplitude over all time, and is not shown.

III. ACPR Calculations

ACPR measurements are typically performed by dividing the power in a narrow band of frequencies (often 30 kHz) in the adjacent channel by either the total power in the main channel, or by the power in a small band of frequencies in the main channel [8]. Since we use discrete

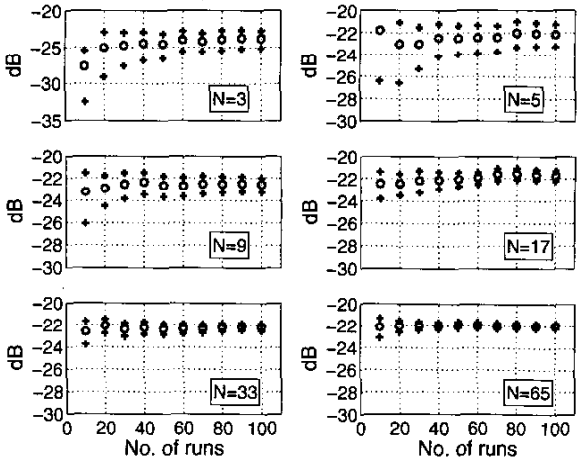

Figure 3: ACPR calculations averaged over increasing numbers of calculations for multisines with different numbers of sinewave components, *N*. Circles are the mean, and crosses are the 95 % confidence intervals.

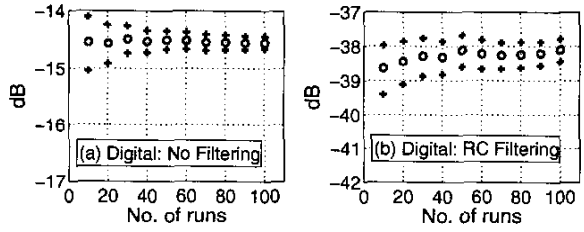

Figure 4: Simulations of pseudorandom digitally modulated signals: (a) no pulse shaping, (b) with raised-cosine pulse shaping. Circles are the mean, and crosses are the 95 % confidence intervals.

tones in the multisine signals, calculation of ACPR over a narrow band does not directly provide an accurate representation of the ACPR (although appropriate scaling could be used to simulate the power in a narrow band in the adjacent channel). We calculated ACPR by dividing the total power in the upper adjacent channel by the power in the main channel. The tone that falls at the edge of the main channel was not shared between the two, but was included in the main channel power only.

The digital signal and two of the multisine cases have random content (pseudorandom bit streams for the digital signal, and random phase and/or magnitude in the other). As a result, convergence was achieved by averaging over a number of different simulations of our ACPR calculations. Figure 3 shows typical results of averaging over increasing numbers of ACPR calculations (runs) for multisines with random magnitude and phase and various numbers of sinewave components. Figure 4 shows the effects of increased averaging for the digital cases. The plot shows the mean value of ACPR as well as the 95 % confidence

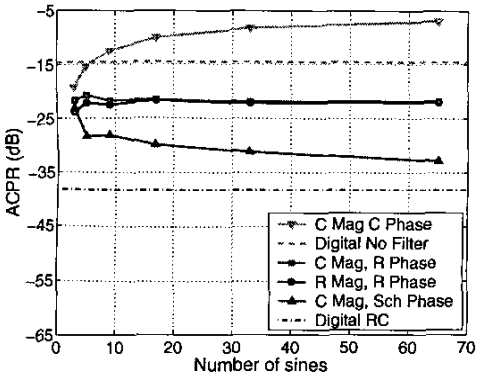

Figure 5: Comparison of ACPR calculations for all four types of multisines and the digital signal with and without raised-cosine pulse shaping. In each case we use the ACPR value found from an average of 10 simulations.

intervals of the mean. We define the 95 % confidence limit by calculating the standard deviation of the mean and applying a coverage factor of two [9].

Note that for multisines with larger numbers of sinewave components, fewer runs are required for convergence. Note also that the variation in the digital signals is smaller than for the multisines, but due to the relatively small number of symbols per simulation, many more runs are necessary for a consistent result.

Figure 5 compares ACPR results for all four multisine excitations and the pseudorandom digital signal with and without raised-cosine pulse shaping. The corresponding time-domain waveforms (after amplification but before limiting) are shown in Fig. 2(a)-(d). 65 sinewave components were used in the multisines. For the cases that involve averaging, the mean of 10 ACPR calculations was used. As expected, the digital signal without pulse shaping (dashed line) has a high ACPR, since the adjacent channel sidebands of the excitation signal (before limiting) are only about 15 dB lower than the main channel maximum [7]. When pulse shaping is applied, the ACPR is greatly reduced, as shown by the dash-dotted line in Fig. 5.

ACPR results for the multisine excitation with either random magnitude and random phase (circles), or with constant magnitude and random phase (squares) are very similar. This can be understood by realizing that changing the phase or magnitude of a sinewave component has a similar effect on the collection of sinewaves, as shown in the signal envelopes of Figs. 2(a) and 2(b).

The multisine excitation signal with constant magnitude and constant phase (inverted triangles) results in underestimation of the power in the main channel, and overestimation of the power in the adjacent channel, as can be seen in Fig. 1(b). Consequently, this sinewave

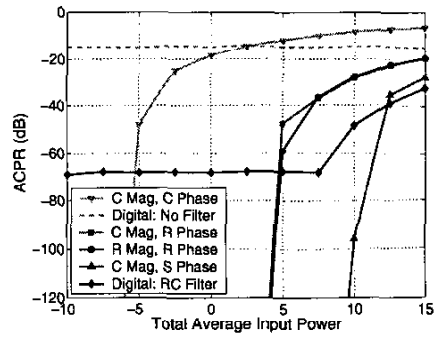

(a)

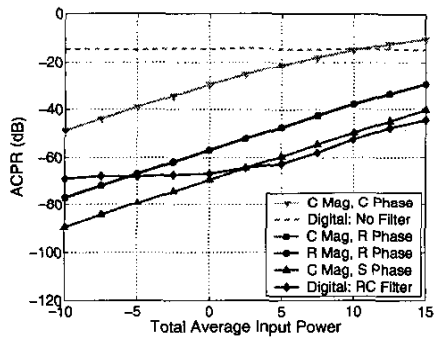

(b)

Figure 6: Effect of input power level variation on ACPR calculations for all four types of multisines and the pseudorandom digital signal with and without raised-cosine pulse shaping. (a) Hard limiting; (b) Soft limiting.

configuration produces the highest ACPR of any of the four. Conversely, the multisine excitation signal with constant magnitude and Schroeder phase results in the lowest ACPR. While the ACPR is still overestimated by approximately 7 dB for our P_{in} of 0.2 W, this signal most closely represents the low PAPR of the digital modulation with raised-cosine pulse shaping, as shown in signal envelopes of Fig. 2(d) and 2(e).

We next swept the input power to show the evolution of the ACPR. For the multisines applied to the hard limiter [Fig. 6(a)], no ACPR occurred below a certain input level, and then increased rapidly when the limiting action starts. The nonzero ACPR of the pulse-shaped digital signal for low power levels is due to the nonzero value of adjacent channel power in the input spectrum, caused by the imperfect, raised-cosine filtering. Again we see that the multisines with random components overestimate the ACPR. Here we also see that the Schroeder multisine underestimates the ACPR for low input power levels. Also, the ACPR of the multisines increases at a rate different from that of the digital signal.

The soft limiter case of Fig. 6(b) shows that the ACPR of the multisines (except for the constant magnitude and phase multisine) increases at nearly the same rate as the digital signal, but with different absolute values.

IV. Conclusion

We used simulation results to compare multisine excitation and pseudorandom digital QPSK excitation for ACPR measurements. Our results demonstrate that caution must be used when trying to characterize digital systems with multisine modulation. Multisines with random magnitude and/or phase may overestimate ACPR of digitally modulated QPSK signals. Multisines with Schroeder phase relationships between sinewave components can improve ACPR estimation; however, we showed that for low power levels, errors may also result.

The importance of accurate estimation of ACPR will be application specific. In some applications, such as robust amplifier design, overestimation of the typical ACPR values may be of benefit. However, in other cases, such as model or system verification, overestimation of ACPR could lead to expensive overdesign of the system.

References

[1] R. Pintelon and J. Schoukens, *System Identification: A Frequency Domain Approach*. New York, NY: IEEE Press, 2001.

[2] W. van Moer, Y. Rolain, and A. Geens, "Measurement based nonlinear modeling of spectral regrowth," *IEEE MTT-S Int. Microwave Symp. Dig.*, pp. 1467-1470, 2000.

[3] G. Simon and J. Schoukens, "Robust broadband periodic excitation design," *IEEE Trans. Instrum. and Measurement*, vol. 49, pp. 270-274, Apr. 2000.

[4] J. C. Pedro and N. B. de Carvalho, "On the use of multitone techniques for assessing RF components' intermodulation distortion," *IEEE Trans. Microwave Theory Tech.*, vol. 47, pp. 2393-2402, Dec. 1999.

[5] R. Hajji, F. Beauregard, and F. M. Ghannouchi, "Multitone power and intermodulation load-pull characterization of microwave transistors suitable for linear SSPA's design," *IEEE Trans. Microwave Theory Tech.*, vol. 45, pp. 1093-1099, July 1997.

[6] J. Verspecht, F. Verbeyst, and M. Vanden Bossche, "Network analysis beyond S-parameters: characterizing and modeling component behaviour under modulated large-signal conditions," *56th ARFTG Conf. Dig.*, pp. 9-12, Dec. 2000.

[7] T. S. Rappaport, *Wireless Communications*. Upper Saddle River, NJ: Prentice Hall PTR, 1996.

[8] D. Vondran, "Making ACPR measurements," *Microwaves and RF*, pp. 79-92, June 2001.

[9] International Organization for Standardization (ISO), "Guide to the Expression of Uncertainty in Measurement." Geneva, Switzerland, 1995.